Vacuolar pH in yeast cells during pseudohyphal growth induced by nitrogen starvation

Koji Makanae[1]

[1]Okayama-shi, Okayama, Japan

Corresponding Author:

Koji Makanae[1]

Email address: maka@kve.biglobe.ne.jp

Abstract

It has been reported that the intracellular pH of the budding yeast *Saccharomyces cerevisiae* is asymmetric between mother and daughter cells, and this asymmetry in pH underlies replicative aging and rejuvenation. *S. cerevisiae* growth morphology changes between the yeast form and pseudohyphal form, according to nutrient availability. A previous study reported that the replicative life span of pseudohyphal form cells is longer than that of yeast form cells in *S. cerevisiae*. However, the intracellular pH of pseudohyphal cells is unknown. To examine the intracellular pH of *S. cerevisiae* cells during pseudohyphal growth, vital staining was performed with neutral red, which is a pH indicator, of cells growing on nitrogen starvation (SLAD) medium. The results showed that the vacuoles of *S. cerevisiae* cells during pseudohyphal growth induced by nitrogen starvation formed polar pH gradients. The relationship between cell size and shape and the neutral red staining patterns suggested that the pH of cell vacuoles during pseudohyphal growth changed from uniformly near pH 6.8 to steep gradients of pH from vacuole ends along the long axis of the cell. The results of time-lapse imaging to examine vacuolar dynamics and neutral red staining suggested that the pH gradients were not formed simply by inheritance of vacuolar contents accompanying vacuolar movements.

Introduction

As a model organism for aging research, the budding yeast *Saccharomyces cerevisiae* is assayed using an index of replicative life span or chronological life span (Longo et al., 2012). Replicative aging in yeast occurs only in mother cells. In budding yeast, mother cells stop dividing after about 20–30 rounds of asymmetric budding, while daughter cells derived from the mother cells are rejuvenated (Mortimer & Johnston, 1959). Although the cause of aging and the mechanism of rejuvenation are unclear, it is reported that the difference in intracellular pH between mother and daughter cells is associated with replicative aging, rejuvenation, and the life span of *S. cerevisiae* (Henderson, Hughes & Gottschling, 2014; Hughes & Gottschling, 2012).

S. cerevisiae occurs in two growth morphological forms, a yeast form and a pseudohyphal form, according to nutrient availability (Madhani, 2000). However, the intracellular pH of pseudohyphal form cells is unknown. A study of heterogeneity in the aging process of *S. cerevisiae* reported that the replicative life span of the pseudohyphal form cells is longer than that of yeast form cells (yeast form cells: on average, 12 buds generated; pseudohyphal form

cells: on average, 23 buds generated) (Lee et al., 2012). Given that this difference in intracellular pH between mother and daughter cells underlies aging and rejuvenation in yeast (Henderson, Hughes & Gottschling, 2014; Hughes & Gottschling, 2012), determination of the intracellular pH of pseudohyphal cells will help elucidate the aging process from the viewpoint of nutrient conditions to eventually contribute more to the understanding of the nature of aging.

This study aimed to investigate the intracellular pH of pseudohyphal *S. cerevisiae* cells. Neutral red is an alkaline dye used as a pH indicator and is widely used for vital staining of cells as it has low toxicity and is capable of staining cells independent of endocytosis (Barbosa & Peters, 1971). We used neutral red, which is useful for examining intracellular pH by vital staining, to examine the intracellular pH of *S. cerevisiae* pseudohyphal cells.

In this study, cells during pseudohyphal growth induced by nitrogen starvation formed steep polar pH gradients in vacuoles from the vacuole ends in *S. cerevisiae*, suggesting that the vacuolar pH changed from a uniform distribution of near pH 6.8 to a bipolar gradient accompanying cell growth, which continued even after first cell division of the new mother cell. Moreover, the results suggested that the polar pH gradients of vacuoles were not formed simply by inheritance of vacuolar contents accompanying vacuolar movement.

Materials & Methods

Table 1. Strains used in this study

Strain	Lineage	Species	Manufacturer
Red Star® Pasteur Red™	Wine yeast	*S. cerevisiae*	Lesaffre
Nisshin Super Kameriya® dry yeast	Baker's yeast	*S. cerevisiae*	Nisshin Foods Inc.
Tokachino Koubo®	Baker's yeast	*S. cerevisiae*	Nippon Beet Sugar Manufacturing Co., Ltd.
Red Star® Côte des Blancs™	Wine yeast	*S. cerevisiae*	Lesaffre

Strains, Media, and Microbiological Techniques

The yeast strains used in this study are listed in Table 1. All strains are commercial products

and were purchased at a nearby supermarket or Amazon.com. YPD (yeast extract/peptone/dextrose) and YP (YPD minus dextrose) were prepared, and yeast manipulations were performed as described by Amberg, Burke & Strathern (2005). Synthetic low ammonia dextrose (SLAD) and synthetic standard ammonia dextrose (SSAD) media were made as described by Gimeno et al. (1992) and Gimeno & Fink (1994). Agar at a concentration of 1% (w/v) was washed with distilled water. The pH of the media was not adjusted. The pH of both SLAD and SSAD agar media, as measured with LAQUAtwin B-712 compact pH meter (HORIBA, Ltd. Kyoto, Japan), was 4.7. Autoclaving was performed with a pressure cooker (Kuripuso clair plus 6L P4310732; T-fal Écully, France) at high heat for 30 min after rising the safety lock pin. Sterilization was confirmed with an indicator tape (SIT-12; Shamrock Labeling Systems Bellwood, IL, USA) that displayed the word "STERILIZED" after the process described above.

Light microscopy

Cells from an overnight culture in liquid YPD were streaked for single cells on solid medium and incubated at room temperature for 2 days (Fig. 2A and 2C), 7.5 days (Fig. 2B and 2D), 1.5 days (Fig. 7, top images, SSAD), 1 week (Fig. 7, top image, Nisshin Super Kameriya® dry yeast, SLAD), or 2 weeks (Fig. 7, top images, Tokachino Koubo® and Red star® Côte de Blancs™, SLAD). Colonies were imaged using a stereomicroscope (LW-602; Wraymer, Inc., Osaka, Japan) fitted with an A20 light stand (Fig. 2A–2D and Fig. 7, top images).

Cells from an overnight culture in liquid YPD were inoculated with a toothpick onto the surface of solid medium, placed a coverslip, and incubated at room temperature for 19 h (Fig. 2E), 23 h (Fig. 2F and 2G), or 33 h (Fig. 2H). The edges of the colonies were imaged using a Wraymer EX-1300 microscope fitted with a 100x oil immersion achromat objective (Fig. 2E–2H).

Cells from an overnight culture in liquid YPD were inoculated with a toothpick onto the surface of solid medium, placed a coverslip, and incubated at room temperature for 1 day. Then, time-lapse imaging was performed manually using a Wraymer EX-1300 microscope fitted with a 100x oil immersion achromat objective (Fig. 5 and 6).

All images were acquired with a Wraymer USB digital camera (WRAYCAM-NF300) and Wraymer Captman software. Cell sizes were measured manually using the elliptical selection tool and scale bars were added to the images using FIJI software (NIH, Bethesda, MD, USA)

(Schindelin et al., 2012). The brightness and contrast of some images were adjusted using PowerPoint presentation software (Microsoft Corporation, Redmond, WA, USA). Room temperature was measured using an Ondotori ease RTR-322 temperature and humidity monitor (T&D Corporation, Nagano, Japan) (Data S1).

Neutral red staining

Cells from an overnight culture in liquid YPD were inoculated with a toothpick onto the surface of an isopore hydrophilic membrane with 0.4 µm pore size (Merck Millipore, Billerica, MA, USA) resting on the solid medium, which was then placed on a 18 x 18 mm coverslip (Matsunami Glass Ind., Ltd., Osaka, Japan) and incubated for 1 day (Fig. 3 and Fig. 7, lower color images) or 1.5 days (Fig. 4). Then, the cells on the isopore membrane were stained with neutral red (Tokyo Chemical Industry Co., Ltd., Tokyo, Japan). Neutral red was dissolved in distilled water at a concentration of 1% (w/v), stored after filter sterilization, and diluted with Dulbecco's phosphate-buffered saline (D-PBS(-)) free of Ca and Mg (Nacalai tesque, Inc., Kyoto, Japan) to a final concentration of 0.02% (w/v) before use. After placing a drop (~15 µL) of 0.02% (w/v) neutral red solution on top of a glass slide, the isopore membrane holding the cells was placed on the glass slide and a drop (~15 µL) of 0.02% (w/v) neutral red solution was applied on top of the isopore membrane further, which was then mounted a 18 x 18 mm coverslip and immediately observed under a light microscope (Fig. 1).

Reagents

Bacto™ Pepton (cat. no. 211677), Bacto™ Yeast extract (cat. no. 212750), Bacto™ Agar (cat. no. 214050), and Difco™ Yeast Nitrogen Base without amino acids and ammonium sulfate (cat. no. 233520) were purchased from BD Biosciences (Franklin Lakes, NJ, USA). D(+)-glucose (cat. no. 049-31165), distilled water (cat. no. 041-16786), and dimethyl sulfoxide (cat. no. 049-07213) were purchased from Wako Pure Chemical Industries, Ltd. (Osaka, Japan).

Ammonium sulfate (cat. no. 01322-00) was purchased from Kanto Chemical Co., Inc. (Tokyo, Japan). Neutral red (product no. N0315) was purchased from Tokyo Chemical Industry Co., Ltd. (Tokyo, Japan). Liquid D-PBS(-) without Ca and Mg (product no. 14249-95) was purchased from Nacalai tesque (Kyoto, Japan).

Results

Morphology of *S. cerevisiae* colonies and cells (Red star® Pasteur Red™) grown on rich media and nutrition starvation media.

Previous studies have reported that glucose starvation causes filamentous growth of haploid yeast (Cullen & Sprague, 2000) and nitrogen starvation in the presence of glucose induces pseudohyphal growth of diploid yeast (Gimeno et al., 1992). Nitrogen starvation in the presence of glucose induces polarized colony formation and pseudohyphal growth of the commercial wine yeast Red star® Pasteur Red™ cells grown on nutrient-depleted media (Fig. 2).

Neutral red staining of Red star® Pasteur Red™ cells growing on membrane-SSAD and membrane-SLAD.

To study the intracellular pH of pseudohyphal cells in *S. cerevisiae*, Red star® Pasteur Red cells from an overnight culture in liquid YPD inoculated on isopore membrane resting on SSAD and SLAD medium (hereinafter, called “membrane-SSAD” and “membrane-SLAD,” respectively) were incubated at room temperature for 1 day, stained with 0.02% (w/v) neutral red/D-PBS(-), and imaged by light microscopy.

Many cells growing on membrane-SSAD contained a spherical red dot inside each vacuole (Fig. 3A–3G). Cells growing on membrane-SLAD showed (1) uniformly red-stained vacuoles, (2) vacuoles contained large red circles occupying the majority of the vacuole, and (3) steep bipolar or steep unipolar gradients of red stain in the vacuoles from the vacuole ends along the long axis of the cell (Fig. 3H–3N). Buds and small cells tended to contain uniformly red-stained vacuoles (Fig. 3L and 3N, Fig. 4F and 4H, buds) and elongated or rod-shaped cells tended to show polar gradients from the vacuole ends (Table 2). Cells possessing multiple vacuoles and pseudohyphae grown on membrane-SLAD showed similar patterns of neutral red staining (Fig. 4).

		Neutral red staining pattern				
		SSAD	SLAD			
		A red dot in each vacuole (n=20)	Uniformly red vacuole (n=20)	Large red circle in vacuole (n=20)	Unipolar gradient from vacuole ends (n=6)	Bipolar gradient from vacuole ends (n=25)
Cell size	Long axis length (μm)	5.84 (0.92)	4.87 (0.84)	5.55 (0.90)	6.97 (1.01)	8.66 (2.11)
	Short axis length (μm)	3.74 (0.57)	3.37 (0.72)	3.79 (0.51)	3.73 (0.36)	4.25 (0.62)
Cell shape	Aspect ratio (long axis length/short axis length)	1.58 (0.22)	1.47 (0.18)	1.47 (0.19)	1.88 (0.31)	2.10 (0.65)

Table 2. Neutral red staining patterns of cells grown on membrane-SSAD and membrane-SLAD.

Values are presented as the mean ± standard deviation in parentheses.

Vacuolar dynamics of Red star® Pasteur Red™ cells grown on SSAD and SLAD medium.

To examine the relationship between the formation of vacuolar pH gradients and vacuolar dynamics, Red star® Pasteur Red™ cells from an overnight culture in liquid YPD were inoculated on SSAD and SLAD medium with a toothpick, placed a coverslip, incubated at room temperature for 1 day, and then examined by time-lapse microscopy (Figs. 5 and 6).

In the yeast and pseudohyphal form cells, vacuoles of the mother cells formed tubular structures towards the daughter buds and supplied vacuoles to the daughter cells (Fig. 5, elapsed time 0, 69, 167, 194 min; Fig. 6, elapsed time 81, 131 min). Some of the vacuoles of the mother cell formed tubular structures towards the vacuole located on the opposite side of the daughter bud (Fig. 5, elapsed time 166 min). In pseudohyphal cells, multiple vacuoles were fused, which were then re-bisected in the cell (Fig. 6, elapsed time 118, 138, 148, 164, 185 min).

These results demonstrated that vacuoles of Red star® Pasteur Red™ cells occurred partly from preexisting vacuoles as well as naturally occurring and repeated fusion and fission both in the yeast and pseudohyphal form cells as described previously (Weisman, Bacallao & Wickner, 1987; De Mesquita, Ten Hoopen & Woldringh, 1991; Weisman, 2003; Klionsky, Herman & Emr, 1990; Li & Kane, 2009).

Strain differences in neutral red staining of cells growing on membrane-SLAD.

To test the generality of the neutral red staining images of Red star® Pasteur Red™ cells grown on membrane-SLAD, three other strains that form polarized colonies on SLAD medium (Nisshin Super Kameriya® dry yeast, Tokachino Koubo® and Red star® Côte de Blancs™) were examined.

Cells of all strains grown on membrane-SLAD for 1 day at room temperature showed a similar pattern of neutral red staining to that of Red star® Pasteur Red™ cells.

Discussion

The purpose of the present study was to examine the intracellular pH of pseudohyphal *S. cerevisiae* cells with neutral red staining. The results of this study showed that during pseudohyphal growth induced by nitrogen starvation, the *S. cerevisiae* cells formed polar pH gradients in vacuoles, suggesting that the uniform distribution of vacuolar pH changed to steep bipolar gradients accompanying cell growth, which continued even after the first cell division. In addition, this finding suggests that the vacuolar pH gradients were not formed simply by inheritance of vacuolar contents accompanying vacuolar movements.

Neutral red staining of cells grown on membrane-SSAD showed a red dot in each vacuole. Meanwhile, cells grown on membrane-SLAD were of various sizes and shapes (round, oval, ellipsoidal, elongated, rod shaped) with various staining patterns (uniformly red vacuoles, vacuoles possessing red circles large enough to fill the vacuole, steep bipolar or steep unipolar gradients of red staining signals in the vacuoles from the vacuole ends along the long axis of the cell) (Figs. 3 and 4).

In cells grown on membrane-SLAD, buds and small cells tended to contain uniformly red-stained vacuole and elongated or rod-shaped cells tended to have polar gradients in the vacuoles from the vacuole ends (Table 2).

The relationship between cell size and the staining pattern suggested that during pseudohyphal growth, the staining pattern of the cell vacuoles changed from uniformly red to the polar gradients from the vacuole ends accompanying cell growth (Figs. 3, 4, and 6).

Time-lapse microscopy of cells grown on SSAD and SLAD medium demonstrated a relationship between the formation of the vacuolar pH gradients and vacuolar dynamics in Red star® Pasteur Red™ cells. Cells grown on both SSAD and SLAD medium showed the formation of tubular structures from the vacuoles of the mother cells towards the daughter buds (Figs. 5 and 6), as described previously (Weisman, Bacallao & Wickner, 1987; De Mesquita, Ten Hoopen & Woldringh, 1991; Weisman, 2003; Klionsky, Herman & Emr, 1990; Li & Kane, 2009). However, neutral red staining of cells grown on membrane-SLAD showed no red-stained tubular structures from the vacuoles, although budding cells were present.

Time-lapse microscopy of cells grown on SLAD showed multiple vacuoles and repeated fusion and bisection in cells during pseudohyphal growth (Fig. 6), as previously described (Veses & Gow, 2008). However, neutral red staining of cells grown on membrane-SLAD showed no red gradient, indicating fusion between red and colorless vacuoles. Even if the gradients occur temporarily by influx of vacuolar contents accompanying vacuole fusion, another mechanism(s) is required to maintain the gradients and form the steep gradients observed in Figs. 3 and 4. These results suggested that the vacuolar gradients are not formed by the transfer of red-stained vacuole contents near pH 6.8 from one vacuole to another.

The cells of three strains other than Red star® Pasteur Red™ formed polarized colonies on SLAD medium. Nisshin Super Kameriya® dry yeast, Tokachino Koubo®, and Red Star® Côte des Blancs™ cells showed similar patterns of neutral red staining as that of Red star® Pasteur Red™ cells (Fig. 7). These results demonstrated that the vacuolar pH gradients observed in Red star® Pasteur Red™ cells growing on membrane-SLAD were not a phenomenon specific to Red star® Pasteur Red™ cells.

There were some limitations to this study that should be acknowledged. First, neutral red acts as a pH indicator, which changes color from red to yellow between pH 6.8 and 8.0. As the range of neutral red is only between pH 6.8 and 8.0, pH not in this range could not be evaluated. Only the pH values near 6.8 (near neutral pH) could be evaluated. (Figs. 3, 4, and

7). Second, it was not possible to image the time-dependent changes of intracellular pH accompanying cell growth because time-lapse microscopy could not be conducted with vital staining and solid culturing simultaneously.

However, as according to previous studies, vacuoles are generally acidic (Martínez-Muñoz and Kane, 2008; Plant et al., 1999; Preston, Murphy & Jones, 1989; Yamashiro et al., 1990; Carmelo, Santos & Sá-Correia, 1997; Diakov & Kane, 2010), we herein considered the vacuoles of cells grown on membrane-SSAD and membrane-SLAD (both were pH 4.7) to be more acidic than the coverage of neutral red (pH 6.8–8.0), while the red regions in the vacuoles were near pH 6.8 and the colorless regions were more acidic than the red regions.

It is reported that vacuole acidification by vacuolar H^+-ATPase (V-ATPase) negatively regulates vacuolar membrane fusion and vacuolar morphology is determined by an equilibrium of vacuolar fission-fusion activity (Baars et al., 2007; Desfougères et al., 2016). Observation of the intracellular pH of cells during pseudohyphal growth using fluorescence-lifetime imaging microscopy (Ogikubo et al., 2011) over time demonstrated a relationship between changes in intracellular pH and vacuolar dynamics accompanying pseudohyphal growth and between vacuolar pH and cytosolic pH; these relationships may help elucidate the mechanism underlying the generation and biological role of vacuolar pH gradients.

Acknowledgement

The author would like to thank Enago (www.enago.jp) for the English language review.

Additional Information and Declarations

Funding

The author received no funding for this work.

Competing Interests

The author declares there are no competing interests.

Author Contributions

Koji Makanae conceived and designed the experiments, performed the experiments, analyzed

the data, contributed reagents/materials/analysis tools, wrote the paper, prepared figures and/or tables, reviewed drafts of the paper.

Data Deposition

The following information was supplied regarding the deposition of related data:

Raw data of time-lapse imaging have been deposited in Figshare:

http://dx.doi.org/10.6084/m9.figshare.4419629

http://dx.doi.org/10.6084/m9.figshare.4419614

Supplemental Information

Supplemental information for this article can be found online at http://dx.doi.org/…

References

Longo, V. D., Shadel, G. S., Kaeberlein, M., & Kennedy, B. (2012). Replicative and chronological aging in Saccharomyces cerevisiae. *Cell metabolism*, *16*(1), 18-31.

Mortimer, R. K., & Johnston, J. R. (1959). Life span of individual yeast cells. *Nature,* 183, 1751 - 1752

Veses, V., & Gow, N. A. (2008). Vacuolar dynamics during the morphogenetic transition in Candida albicans. *FEMS yeast research*, *8*(8), 1339-1348.

Henderson, K. A., Hughes, A. L., & Gottschling, D. E. (2014). Mother-daughter asymmetry of pH underlies aging and rejuvenation in yeast. *Elife*, *3*, e03504.

Hughes, A. L., & Gottschling, D. E. (2012). An early age increase in vacuolar pH limits mitochondrial function and lifespan in yeast. *Nature*, *492*(7428), 261-265.

Madhani, H. D. (2000). Interplay of intrinsic and extrinsic signals in yeast differentiation. *Proceedings of the National Academy of Sciences*, *97*(25), 13461-13463.

Lee, S. S., Vizcarra, I. A., Huberts, D. H., Lee, L. P., & Heinemann, M. (2012). Whole lifespan microscopic observation of budding yeast aging through a microfluidic dissection platform. *Proceedings of the National Academy of Sciences*, *109*(13), 4916-4920.

Barbosa, P., & Peters, T. M. (1971). The effects of vital dyes on living organisms with special reference to methylene blue and neutral red. *The Histochemical Journal*, *3*(1), 71-93.

Schindelin, J., Arganda-Carreras, I., Frise, E., Kaynig, V., Longair, M., Pietzsch, T., ... & Tinevez, J. Y. (2012). Fiji: an open-source platform for biological-image analysis. *Nature methods*, *9*(7), 676-682.

Amberg, D. C., Burke, D. J., & Strathern, J. N. (2005). Methods in Yeast Genetics: A Cold Spring Harbor Laboratory Course Manual, 2005 Edition (Cold Spring).

Gimeno, C. J., Ljungdahl, P. O., Styles, C. A., & Fink, G. R. (1992). Unipolar cell divisions in the yeast S. cerevisiae lead to filamentous growth: regulation by starvation and RAS. Cell, 68(6), 1077-1090.

Gimeno, C. J., & Fink, G. R. (1994). Induction of pseudohyphal growth by overexpression of PHD1, a Saccharomyces cerevisiae gene related to transcriptional regulators of fungal development. Molecular and Cellular Biology, 14(3), 2100-2112.

Cullen, P. J., & Sprague, G. F. (2000). Glucose depletion causes haploid invasive growth in yeast. *Proceedings of the National Academy of Sciences*, *97*(25), 13619-13624.

Weisman, L. S., Bacallao, R., & Wickner, W. (1987). Multiple methods of visualizing the yeast vacuole permit evaluation of its morphology and inheritance during the cell cycle. *The Journal of Cell Biology*, *105*(4), 1539-1547.

De Mesquita, D. S. G., Ten Hoopen, R., & Woldringh, C. L. (1991). Vacuolar segregation to the bud of Saccharomyces cerevisiae: an analysis of morphology and timing in the cell cycle. *Microbiology*, *137*(10), 2447-2454.

Weisman, L. S. (2003). Yeast vacuole inheritance and dynamics. *Annual review of genetics*, *37*(1), 435-460.

Klionsky, D. J., Herman, P. K., & Emr, S. D. (1990). The fungal vacuole: composition, function, and biogenesis. *Microbiological reviews*, *54*(3), 266-292.

Li, S. C., & Kane, P. M. (2009). The yeast lysosome-like vacuole: endpoint and crossroads. *Biochimica et Biophysica Acta (BBA)-Molecular Cell Research*, *1793*(4), 650-663.

De Mesquita, D. S. G., Ten Hoopen, R., & Woldringh, C. L. (1991). Vacuolar segregation to the bud of Saccharomyces cerevisiae: an analysis of morphology and timing in the cell cycle. *Microbiology*, *137*(10), 2447-2454.

Preston, R. A., Murphy, R. F., & Jones, E. W. (1989). Assay of vacuolar pH in yeast and identification of acidification-defective mutants. *Proceedings of the National Academy of Sciences*, *86*(18), 7027-7031.

Plant, P. J., Manolson, M. F., Grinstein, S., & Demaurex, N. (1999). Alternative mechanisms of vacuolar acidification in H+-ATPase-deficient yeast. *Journal of Biological Chemistry*, *274*(52), 37270-37279.

Yamashiro, C. T., Kane, P. M., Wolczyk, D. F., Preston, R. A., & Stevens, T. H. (1990). Role of vacuolar acidification in protein sorting and zymogen activation: a genetic analysis of the yeast vacuolar proton-translocating ATPase. *Molecular and Cellular Biology*, *10*(7), 3737-3749.

Martínez-Muñoz, G. A., & Kane, P. (2008). Vacuolar and plasma membrane proton pumps collaborate to achieve cytosolic pH homeostasis in yeast. *Journal of Biological Chemistry*, *283*(29), 20309-20319.

Carmelo, V., Santos, H., & Sa-Correia, I. (1997). Effect of extracellular acidification on the activity of plasma membrane ATPase and on the cytosolic and vacuolar pH of Saccharomyces cerevisiae. *Biochimica et Biophysica Acta (BBA)-Biomembranes*, *1325*(1), 63-70.

Diakov, T. T., & Kane, P. M. (2010). Regulation of vacuolar proton-translocating ATPase activity and assembly by extracellular pH. *Journal of Biological Chemistry*, *285*(31), 23771-23778.

Baars, T. L., Petri, S., Peters, C., & Mayer, A. (2007). Role of the V-ATPase in regulation of

the vacuolar fission–fusion equilibrium. *Molecular biology of the cell*, *18*(10), 3873-3882.

Desfougères, Y., Vavassori, S., Rompf, M., Gerasimaite, R., & Mayer, A. (2016). Organelle acidification negatively regulates vacuole membrane fusion in vivo. *Scientific reports*, *6*.

Ogikubo, S., Nakabayashi, T., Adachi, T., Islam, M. S., Yoshizawa, T., Kinjo, M., & Ohta, N. (2011). Intracellular pH sensing using autofluorescence lifetime microscopy. *The Journal of Physical Chemistry B*, *115*(34), 10385-10390.

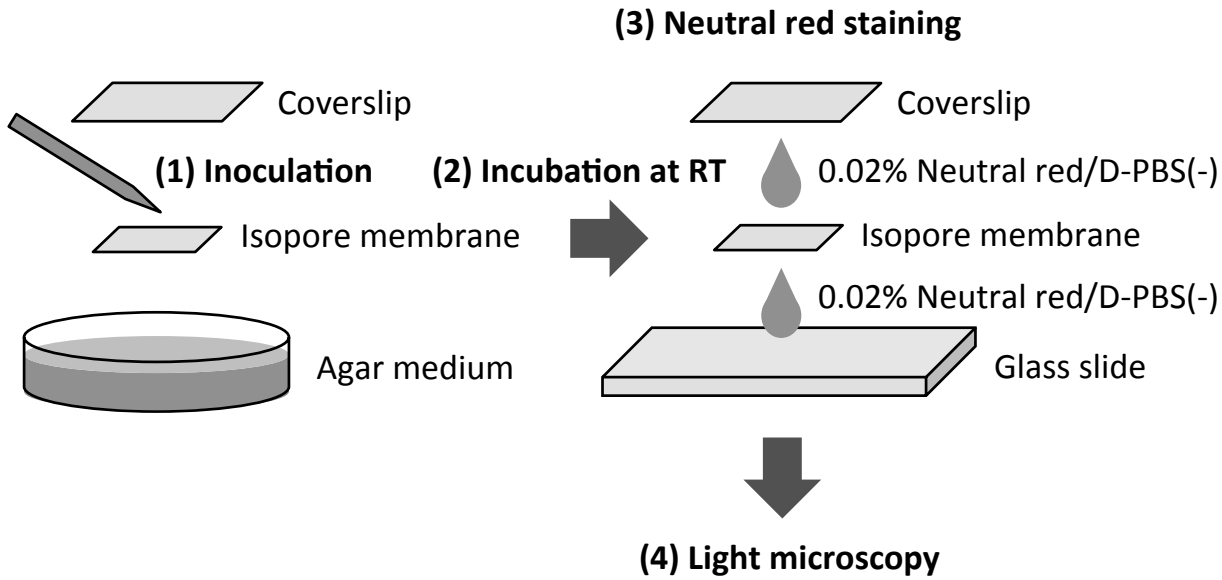

Fig. 1. Diagram of the experimental procedure for neutral red staining of cells grown on an isopore membrane resting on solid medium.

(1) Inoculation of suspended cells from an overnight culture in liquid YPD on the surface of an isopore membrane resting on solid medium using a toothpick.

(2) Incubation at room temperature for 1–1.5 days.

(3) Neutral red staining of cells grown on an isopore membrane on a glass slide.

(4) Imaging by light microscopy with a 100x oil immersion objective.

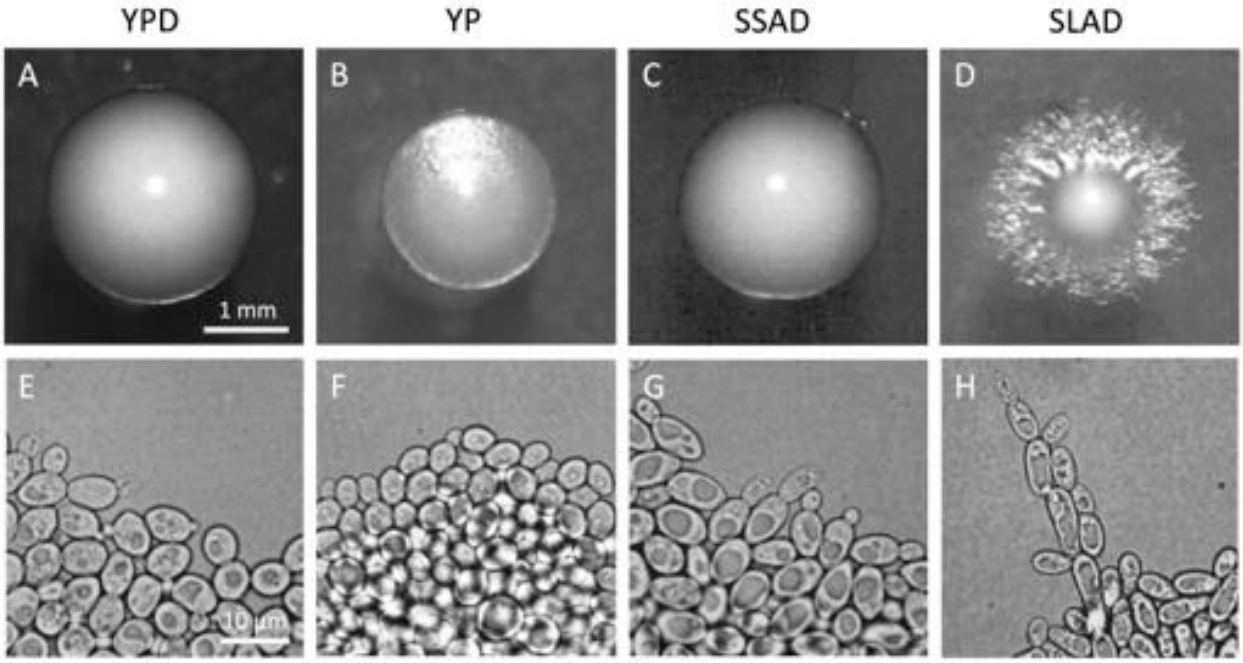

Fig. 2. Morphology of Red star® Pasteur Red™ colonies and cells growing on YPD, YP, SSAD, and SLAD medium.

(A–D) Single colonies of Red star® Pasteur Red™ cells growing on YPD, YP, SSAD, and SLAD medium. Scale bars in A, B, C, and D, 1 mm. (E–H) The edge of a colony of Red star® Pasteur Red™ cells grown on YPD, YP, SSAD, and SLAD medium. Scale bars in E, F, G, and H, 10 µm.

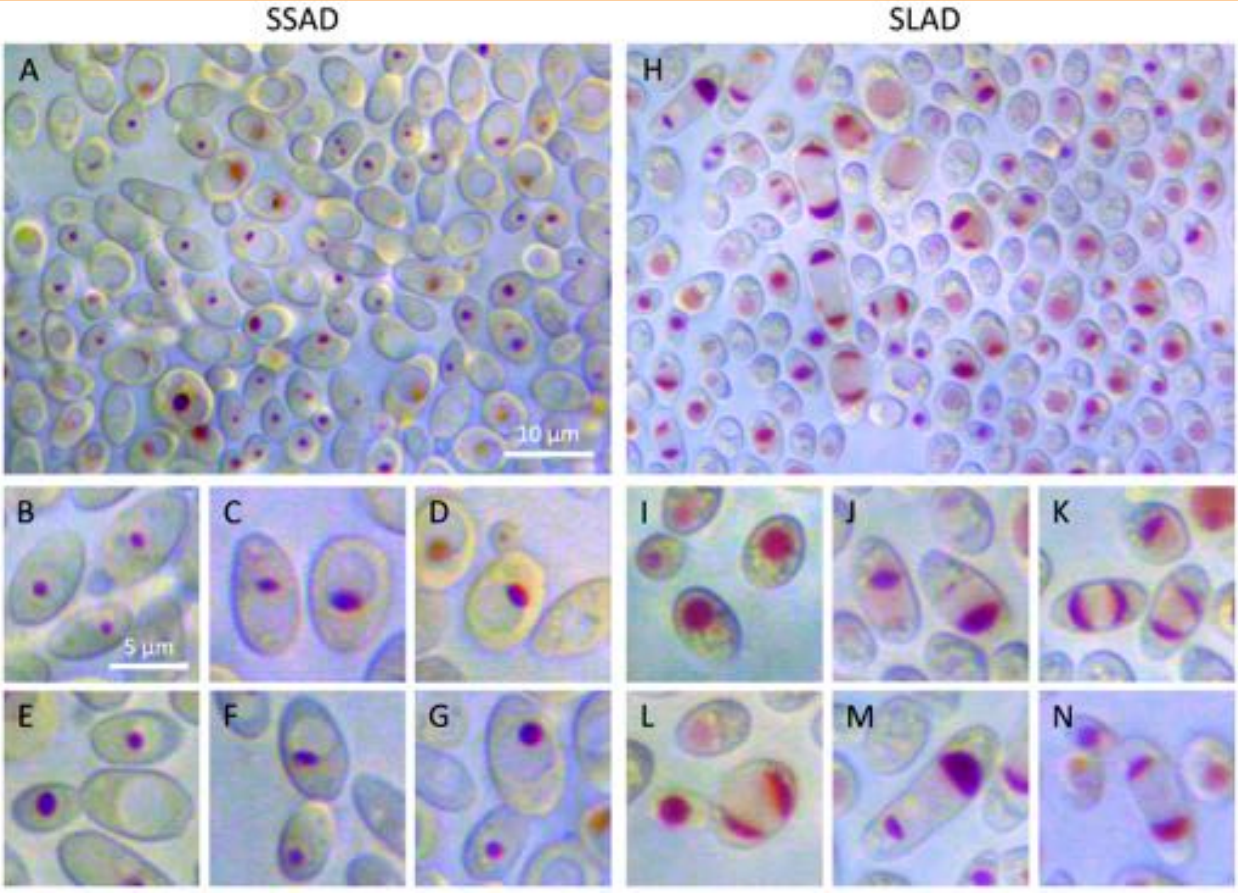

Fig. 3. Neutral red staining of Red star® Pasteur Red™ cells grown on membrane-SSAD and membrane-SLAD.

Representative images of Red star® Pasteur Red™ cells stained with neutral red that were grown on membrane-SSAD (A–G) or membrane-SLAD (H–N) for 1 day at room temperature. Scale bar, 10 µm (A and H) and 5 µm (B–G and I–N).

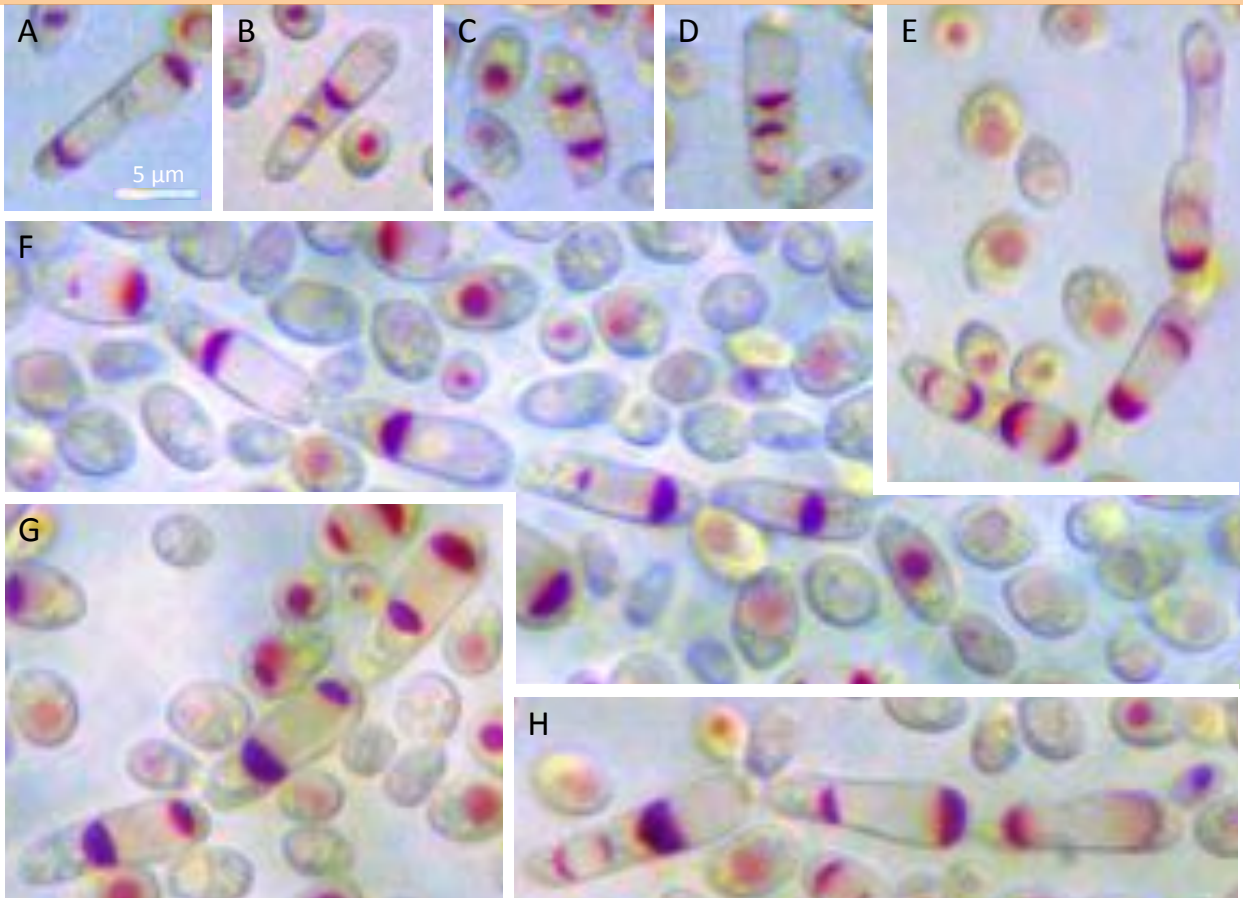

Fig. 4. Neutral red staining of Red star® Pasteur Red™ cells with multiple vacuoles and pseudohyphae grown on membrane-SLAD.

Representative images of pseudohyphal Red star® Pasteur Red™ cells stained with neutral red that were grown on membrane-SLAD. The scale bar is for all images and represents 5 µm.

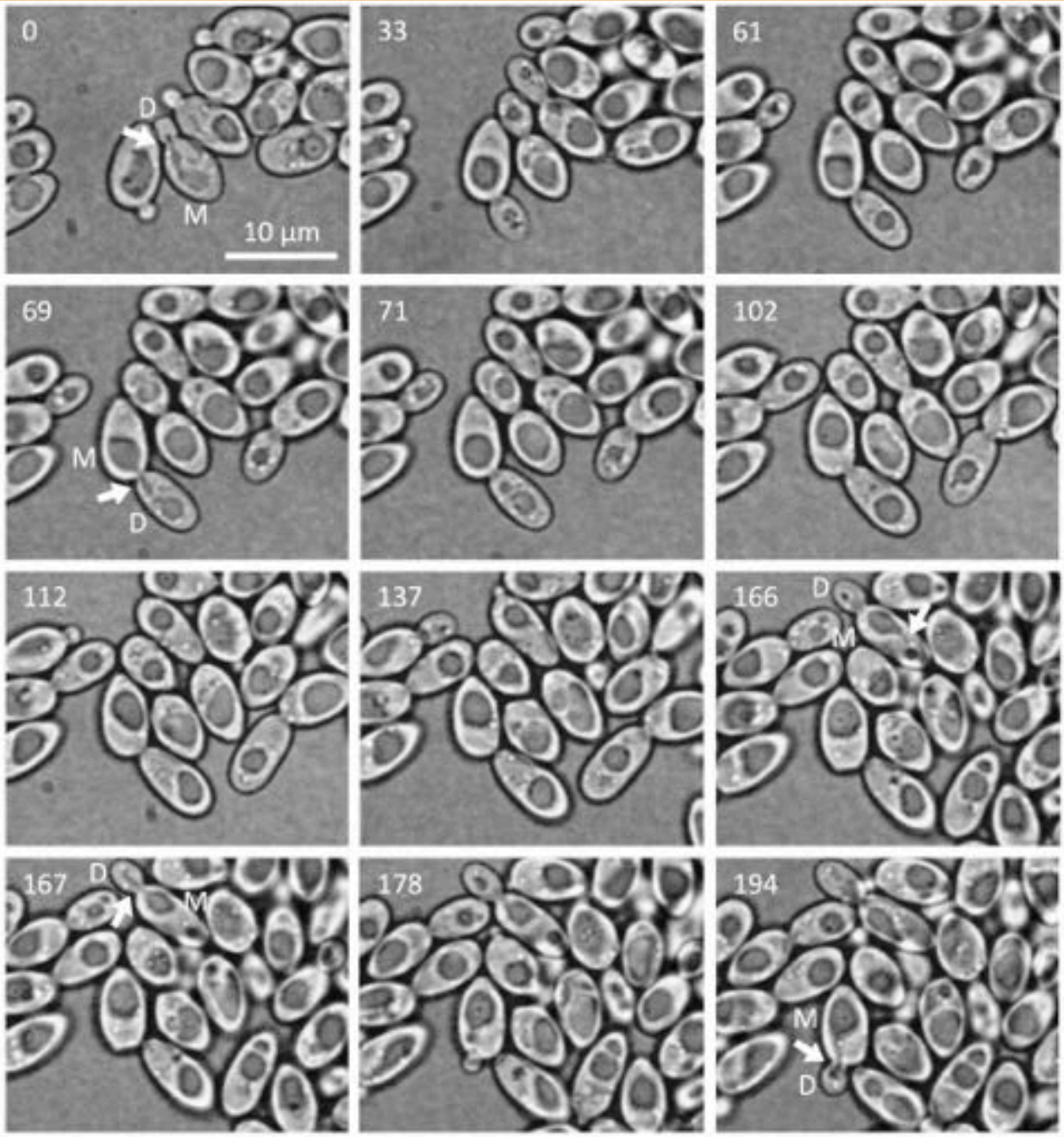

Fig. 5. Time-lapse microscopy images of Red star® Pasteur Red™ cells grown on SSAD medium.

Images of time-lapse microscopy of Red star® Pasteur Red™ cells grown on SSAD medium for 1 day at room temperature. White arrows point to tubular vacuoles. M: mother; D: daughter.

Elapsed time (min) is shown in the upper left-hand corner in each frame. Scale bar, 10 µm.

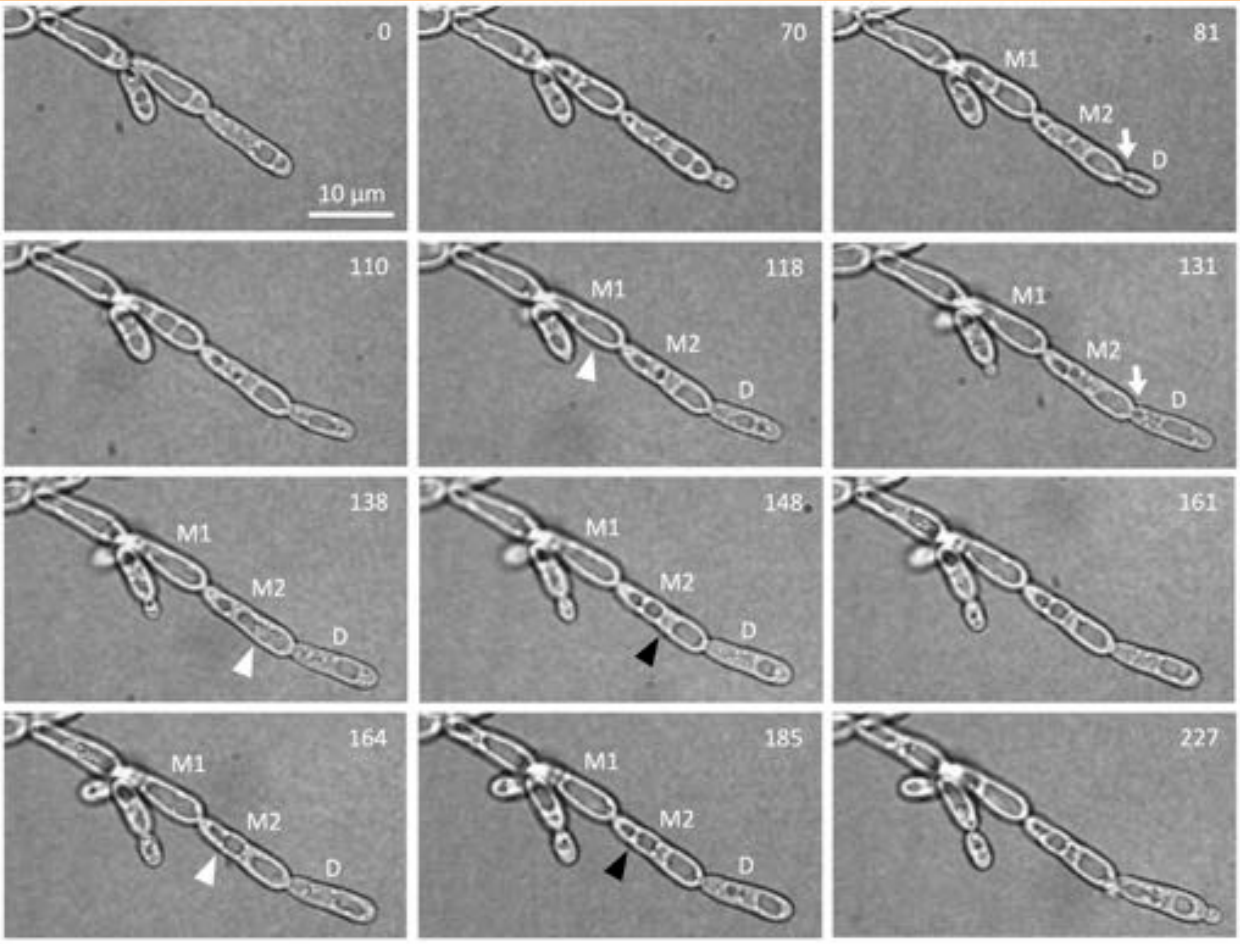

Fig. 6. Time-lapse microscopy images of Red star® Pasteur Red™ cells grown on SLAD medium.

Images of time-lapse microscopy of Red star® Pasteur Red™ cells grown on SLAD medium for 1 day at room temperature. The white arrow points to a tubular vacuole. The white arrowheads point to fusion of segregated vacuoles. The black arrowheads point to bisection of vacuoles. M1: mother; M2: daughter cell of the mother (M1); D: daughter cell of the mother cell (M2). Elapsed time (min) is shown in the upper right-hand corner in each frame. Scale bar, 10 µm.

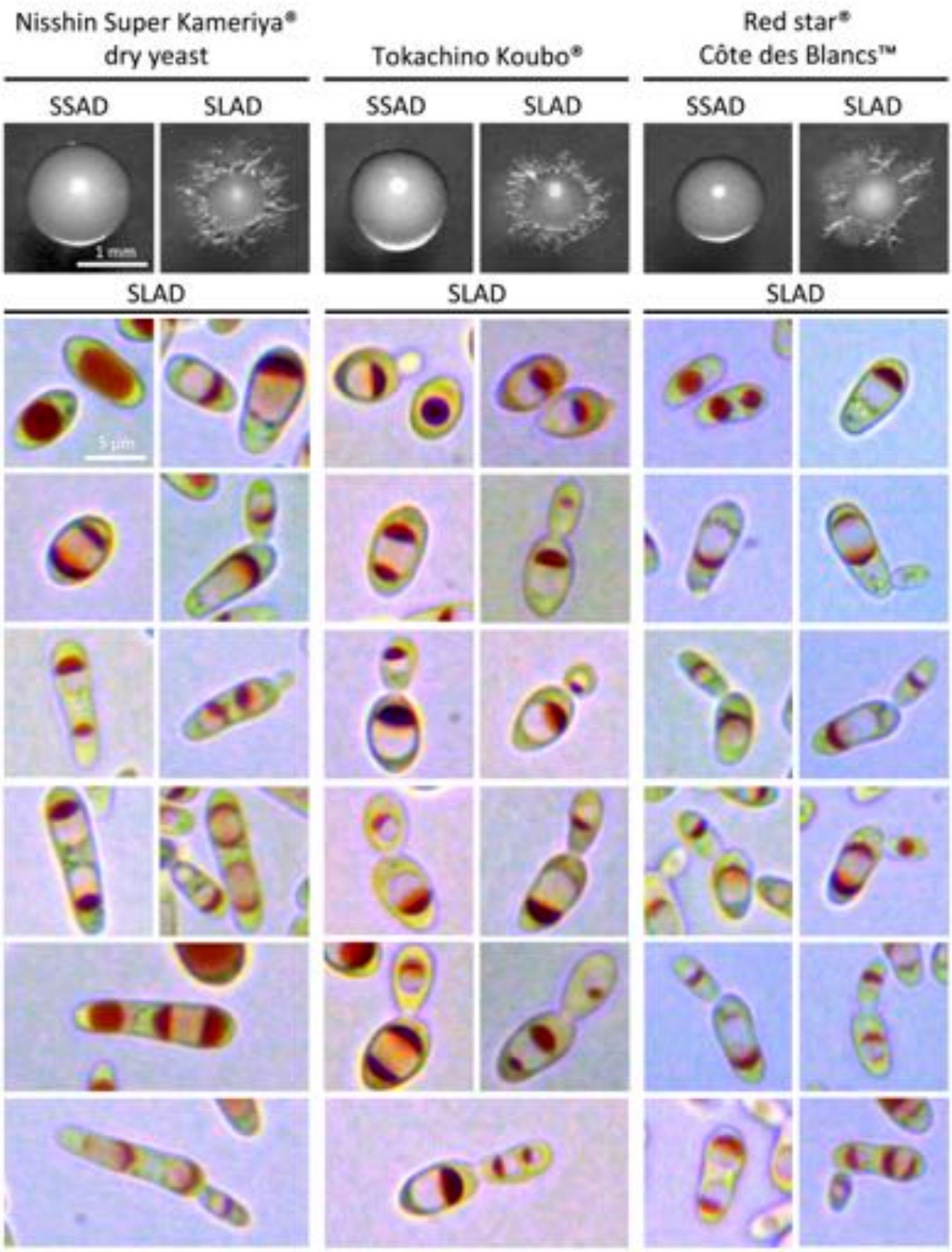

562
563
564
565
566

Fig. 7. Neutral red staining of Nisshin Super Kameriya® dry yeast, Tokachino Koubo®, and Red star® Côte de Blancs™ cells grown on membrane-SLAD.

Single colonies of Nisshin Super Kameriya® dry yeast, Tokachino Koubo®, and Red star® Côte de Blancs™ cells grown on SSAD and SLAD medium (top images). Representative microscopy images of Nisshin Super Kameriya® dry yeast, Tokachino Koubo®, and Red Star® Côte des Blancs™ cells stained with neutral red grown on membrane-SLAD for 1 day at room temperature (lower color images). Scale bar, 1 mm (top images) and 5 μm (lower color images).